Map of Energy

- Light
- Heat
- Mechanical energy
  - Kinetic energy
  - Potential energy

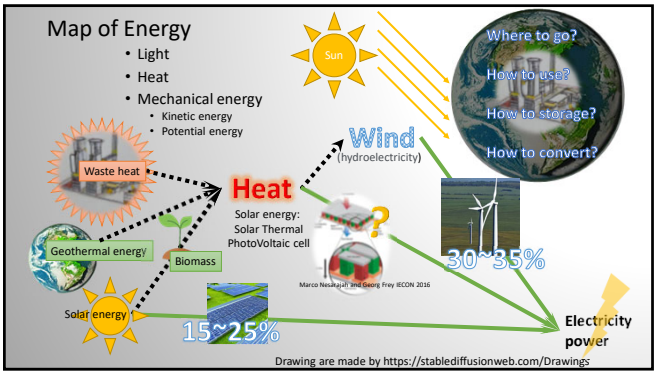

Waste energy from thermal engines:

- According to 2nd law of thermodynamics, the maximum efficiency of heat transformed to work would be the Carnot cycle as follow,

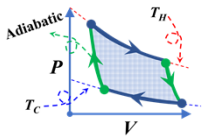

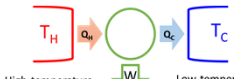

- Efficiency of Carnot cycle: $\eta_C = \frac{T_H - T_C}{T_H}$
- Example:
  - T_H = 1000 K (~727 °C), T_C = 600 K (~327 °C) ⇨ η_C = 0.4

Review

Abram F. Ioffe

Ioffe (1957)
Figure of merit

$$\eta = \left\{\frac{(T_H - T_C)}{T_H}\right\}\left\{\frac{(1+ZT)^{0.5}}{T_C/T_H + (1+ZT)^{0.5}}\right\},$$

Carnot cycle | Material factor

$$ZT = \frac{S^2\sigma}{\kappa}T$$

$$\kappa = \kappa_e + \kappa_{ph}$$

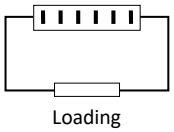

Loading

The Seebeck Effect

Heat → Electricity

1821	T . J . Seebeck Seebeck effect:	Temperature gradient generates electrical potential $V = \alpha_{AB} \cdot \Delta T$

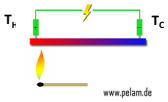

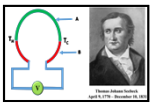

S= Seebeck Coefficient (V/K)

$\Delta V = S \times \Delta T$

5

Practical Applications: Thermocouple

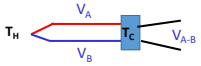

If A is P type, B is N type

$V_{A-B} = (S_A - S_B) \times (T_H - T_C)$

For example:
K type includes
P type Chromel (90% Ni+ 10 % Cr) +21.7 μV/K
N type Alumel (95% Ni+2% Mn+2% Al+1% Si) -17.3 μ V/K

40 uV /K output

6

Peltier Effects

Electricity → Temperature Gradient

1834	J . C . A Peltier Peltier effect:	Applied voltage creates Temperature gradient $\pi_{AB} = \frac{Q}{I}$

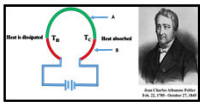

7

Thomson Effects

Heat ⇆ electricity

1821	T . J . Seebeck Seebeck effect:	Temperature gradient generates electrical potential $V = \alpha_{AB} \cdot \Delta T$
1834	J . C . A Peltier Peltier effect:	Applied voltage creates Temperature gradient $\pi_{AB} = \frac{Q}{I}$
1855	湯姆森效應 Thomson effect	$\Pi_{AB} = T\,\alpha_{AB}$

Working Principle

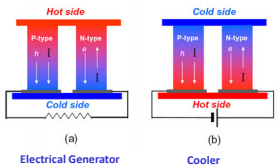

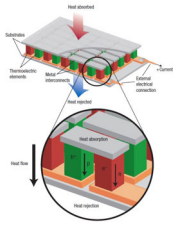

P-N Pairs

Marco Nesarajah and Georg Frey IECON 2016

https://www.youtube.com/watch?v=21EC0Z0imw

The Advantages of Thermoelectric Devices

- ✓No moving parts (Low-noise operation)
- ✓Solid-state elements (Less maintenance)
- ✓High Scalability
- ✓High reliability: long lifetimes
- ✓Reversable operation: Easy switching from cooling to heating mode

TE Applications

Thermoelectric Generators

Industrial Waste-Heat

Vehicle exhaust BMW-BSST

Wrist watch SEIKO

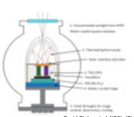

David Ginley *et al.* NREL, JPL

Solar Thermoelectric Generators

Wearable TEG

Hybrid Solar Thermal System/GMZ

Application 1: Thermoelectric Generators for Space - Radioisotope Thermoelectric Generators (RTG)

For Space Exploration missions, the electrical power is provided by converting the heat from a **Pu238 (Plutonium)** instead of sunlight have been used by NASA in a variety of missions such as Apollo, Pioneer, Viking, Voyager, Galileo, and Cassini.

The power sources **for Voyager** are still operating, allowing the spacecraft to continue to make scientific discoveries after **over 35 years of operation**.

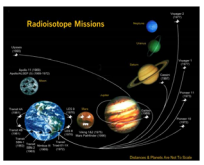

NASA Call for a new generation of RTG

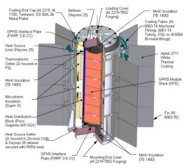

California Institute of Technology
http://www.thermoelectrics.caltech.edu/thermoelectrics/history.html

Thermoelectric Generators

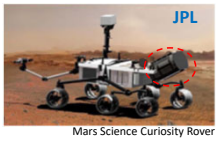

Mars Science Curiosity Rover

NASA/JPL

Radioisotope Thermometric Generator (RTG)

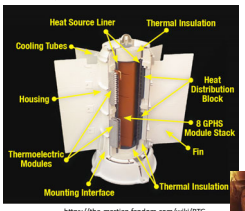

https://the-martian.fandom.com/wiki/RTG

14

Cooler

Driven by an applied potential , electrons (holes) absorb heat from the lattice at the cold side, and reject heat to the lattice at the hot side (Refrigeration)

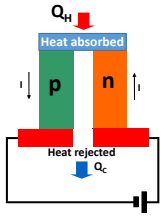

- ✓No vibration
- ✓Less maintenance
- ✓Small size
- ✓High reliability
- ✓Heat manageable

15

TE Cooler: advantage over TEG with driving current I, Δ T > 40 K

Local cooling on chip

"GPD optoelectronics corp"

InGaAs Thermoelectric Cooled IR Photodiodes

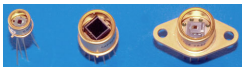

Medical-Grade Refrigerator

"Phononic"
https://phononic.com

https://ibywind.com/

16

Seebeck Coefficient

材料	材料	導電率 (S/m)	西貝克係數 (μV/K)
金屬元素	Au	4.1×10^7	1.7
	Cr	7.9×10^6	18
半導體	Si	1000	400
	Se	8.3×10^6	900
半導體化合物	P-type $Bi_{1.5}Sb_{0.5}Te_3$	5×10^4	185
	N-type $Bi_2Te_{2.7}Se_{0.3}$	1×10^5	-230

Timeline of selected thermoelectric materials

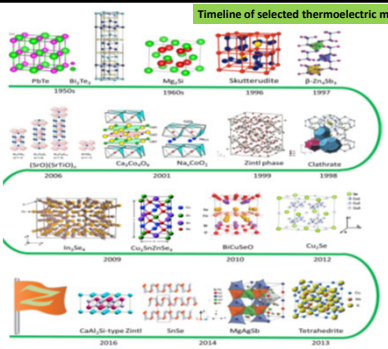

Source: *Materials Today Physics*, 1, 50 (2017)

18

TE development in history

Year	Alloy	ZT		Authors
		P-type	N-type	
1955-1960	Bi_2Te_3	1.0,	0.7	~300 K
1997	Zn_4Sb_3	1.3		670 K, T.Caillat et al
2003	PbTe/PbSeTe	1.6		300 K, Harman et al
2001	Bi_2Te_3/Sb_2Te_3	2.4		Venkatasubramanian, Nature 413, 597
2012	Na:PbTe 2%SrTe	2.2		Biswas et al
2014	SnSe crystal	2.6 ?		Zhao et al
2020	$Ge_{1-x}Bi_xTe$ crystal	1.9		Y. Y. Chen's group
2020	$Ge_{1-x}Sb_xTe$ crystal	2.2		Y. Y. Chen's group

19

Efficiency vs. ZT

$$Q_H = \kappa\Delta T + ST_H I + \frac{I^2 R}{2}$$

$$W = I^2 R_L = \frac{S^2 \Delta T^2 R_L}{(R + R_L)^2}$$

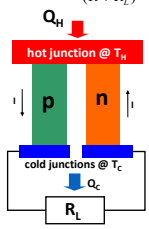

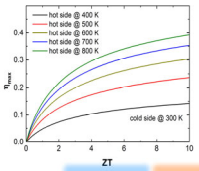

$$ZT = \frac{S^2\sigma}{\kappa} T$$

Carnot Cycle | Material factor < 1

$$\eta = \frac{W}{Q_H} = \ldots = \frac{\Delta T}{T_H} \frac{\sqrt{1+ZT}-1}{\sqrt{1+ZT}+T_C/T_H}$$

Real-world applications require
η > 0.1 (economically …)

20

Dimensionless figure-of-merit ZT

$$ZT = \frac{\sigma S^2}{\kappa} T$$

S : Seebeck coefficient
σ : Electrical conductivity
κ : Thermal conductivity
T :Absolute temperature

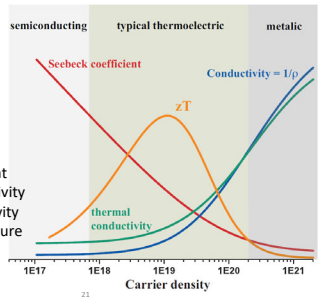

21

TE generators vs. Conventional engines

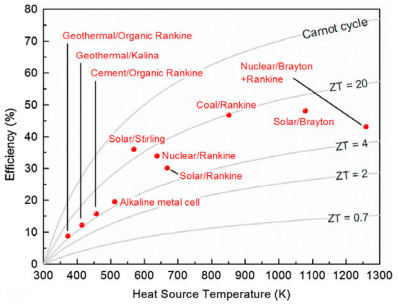

Data source: *Materials Science & Engineering* R (2019) : https://doi.org/10.1016/j.mser.2018.09.001

22

p-type Thermoelectric Materials

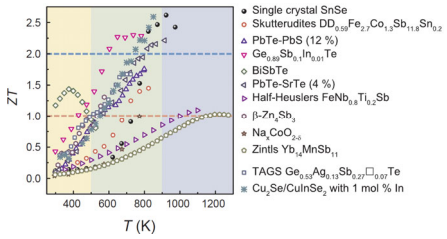

Progress in Materials Science 97 (2018) 283

23

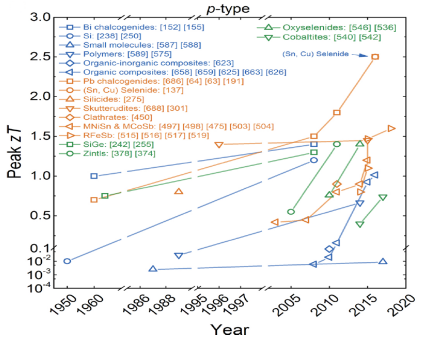

Data source: *Materials Science & Engineering* R (2019) : https://doi.org/10.1016/j.mser.2018.09.001

24

n-type Thermoelectric Materials

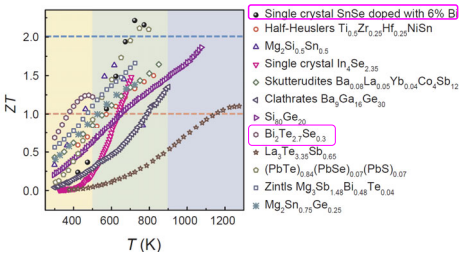

Progress in Materials Science 97 (2018) 283

25

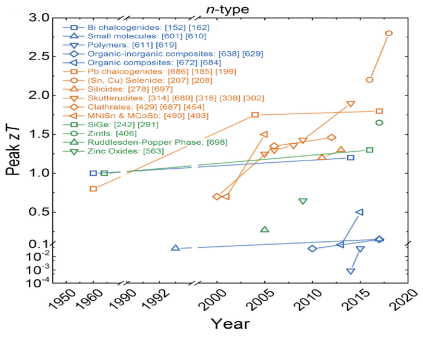

Data source: *Materials Science & Engineering* R (2019) : https://doi.org/10.1016/j.mser.2018.09.001

26

Common characteristics of high-performance TE materials

1. An optimum band gap that is large enough to inhibit the excitation of minority carriers
   → narrow band gap, covalent bonding
2. Lower thermal conductivity
   → compounds formed between heavier elements
3. Materials with more symmetrical crystal structures tend to have better electronic properties than others with lower symmetry
4. The compound could be heavily doped.
5. Complex structures with many atoms in the unit cell
   → so the heat-carrying phonon is damped.

ex: Bi_2Te_3, PbTe, GeTe, SnSe, $Si_{1-x}Ge_x$

27

Major challenge in thermoelectrics

" higher performance, non-toxic and sustainable "

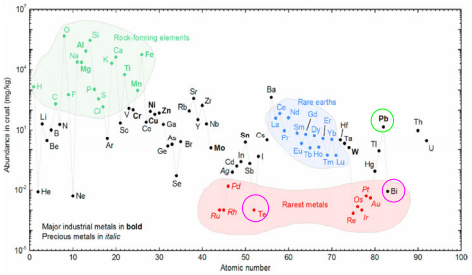

Data source: *Materials Science & Engineering* R (2019) : https://doi.org/10.1016/j.mser.2018.09.001

28

II. Stratagem of enhancing ZT

- ✓ **Electronic band structure** — band convergence $ZT = \frac{\sigma S^2}{\kappa}T$
- ✓ **Reduction in thermal conductivity** $ZT = \frac{\sigma S^2}{\kappa}T$
  Intrinsically low lattice κ , Defect Engineering
- ✓ **Synergistically manipulating charge and phonon transports** $ZT = \frac{\sigma S^2}{\kappa}T$
- ✓ **3D charge and 2D phonon transports** $ZT = \frac{\sigma S^2}{\kappa}T$

29

Mechanisms for *S* enhancement in bulk

Mechanism	Theory	Simulation	Material
Carrier filtering	[1999] Thermionic emission current in heterostructures	[2008] Band bending at PbTe/metal interfaces	[2009] Bulk(PbTe) [2010] Bulk(skutterudite) [2011] Bulk(TAGS) [2011] Pt-Sb_2Te_3
Resonant State	[1956] Virtual bound (resonant) state by doping [1996] DOS engineering	[2006] Doped PbTe	[2008] Tl-doped PbTe [2009] Sn-doped Bi_2Te_3

$$ZT = \frac{S^2\sigma}{\kappa}T$$

Carrier filtering effect

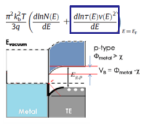

Resonant state

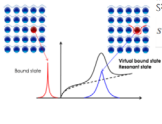

If E_F is tuned to near a peak in DOS, $S^2\sigma$ would be sharply increased!

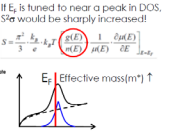

S.V. Faleev, *Phys. Rev. B* 77, 214304 (2008) J. Friedel, *J. Physics*, 1956 ORNL, PNAS, 1996

30

Stratagem of enhancing ZT

- ✓ **Electronic band structure** — band convergence
- ✓ Reduction in thermal conductivity
  Intrinsically low lattice κ , Defect Engineering
- ✓ Synergistically manipulating charge and phonon transports
- ✓ 3D charge and 2D phonon transports

31

Thermoelectric quality factor (*B*)

$$\sigma = ne\mu = \frac{ne^2\tau}{m_b^*} \qquad \mu \propto \frac{1}{m_b^*}$$

$$B \propto \frac{N_v}{m_I^* \kappa_L}$$

$$S \propto m_d^* \qquad m_d^* = N_v^{2/3} m_b^*$$

$$ZT = \frac{S^2\sigma}{\kappa} T$$

$$S \sim \frac{8\pi^2 k_B^2}{3eh^2} m_d^* T \left(\frac{\pi}{3n}\right)^{2/3}$$

μ : carrier mobility (in $cm^2 V^{-1}s^{-1}$)
m_d*: Density of states effective mass
m_I* : Inertial effective mass
m_b* : band effective mass
N_v : the number of band valleys
κ_L : latteice thermal conductivity

32

Importance of band convergence

PbTe, PbSe, GeTe, SnSe, SnTe, $Mg_2Sn_{1-x}Ge_x$.....

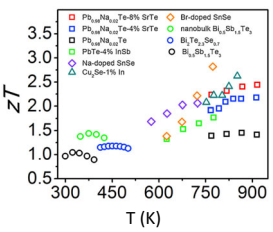

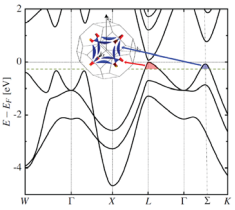

Fermi surface and band structure
Materials Project https://materialsproject.org
The schematic *L* (red) and
Σ (blue) carrier pockets

33

Convergence of electronic bands for PbTe

G. Jeffrey Snyder *et al*. Nature, 473, 66 (2011)

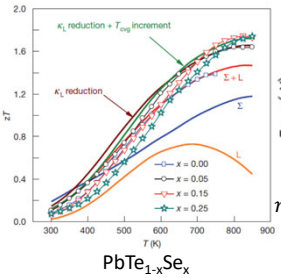

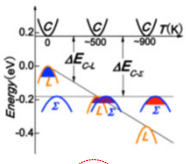

$$m_{DOS}^* = N_v^{2/3} m_{band}^*$$

Valley degeneracy

$PbTe_{1-x}Se_x$

34

Heavy and Light holes in PbTe

Valence Band Maximum is at *L* point
- "Light Band" $N_V = 4$, $m_b^* = 0.14\, m_e$

(8 half pockets at the L point lead to $N_V = 4$)

Second valence band occurs at Σ line
- "Heavy Band" $N_V = 12$, $m_b^* = 0.28\, m_e$

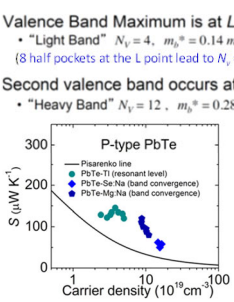

$$S = \frac{8\pi^2 k_B^2}{3eh^2} m_{DOS}^* T \left(\frac{\pi}{3n}\right)^{2/3}$$

$$\sigma = ne\mu$$

$$ZT = \frac{\sigma S^2}{\kappa} T$$

35

Tuning the reduced Fermi level by doping enables an optimization of *zT* - *Single Band Model of Thermoelectricity*

zT for different *B* factor

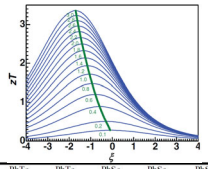

peak *zT* as a function of *B*

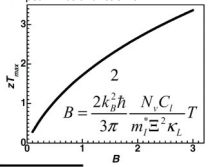

	PbTe	PbTe	PbSe	PbSe	PbS	$Si_{0.7}Ge_{0.3}$	Bulk Si
type	n	P(L)	n	P(L)	n	n	n
$T_{operate}$	800	800	850	850	900	1000	1000
$\mu_0 m^{*3/2}$							
N_v	4	4	4	4	4	6	6
C_l (GPa)	71	71	91	91	111	150	180
m_I^*	0.15	0.17	0.17	0.17	0.25	0.27	0.26
Ξ	23	28	27	38	28	15	15
κ_L	0.75	0.75	0.65	0.65	0.95	4	45
B	0.7	0.4	0.67	0.33	0.39	0.68	0.07

$$B = \frac{2k_B^2\hbar}{3\pi} \frac{N_v C_l}{m_I^{*2} \Xi^2 \kappa_L} T$$

k_B: Boltzmann constant
h: Planck constant
N_v: number of degenerated valleys
C_l: average longitudinal elastic moduli
m_I*: inertial effective mass
Ξ: deformation potential coefficient
ξ: reduced Fermi level

Adv. Mater. **24**, 6125 (2012)

36

	Bulk Ge	Mg_2Si	$Mg_2Si_{0.6}Sn_{0.4}$	SnTe	SnSe	Cu_3SbSe_4	Bi_2Te_3
type	n	n	n	p(L)	n	p	n (//c)
$T_{operate}$	1000	700	700	773	750	673	400
$\mu_0 m^{*3/2}$							
N_v	4	3	6	4	2	3	6
C_l	160	120	100	58	58	80	71
m_I^*	0.12	0.5	0.8	0.09	0.47	0.7	0.1
Ξ	20	15	13	28	21	14	24
κ_L	18	3	1.5	1.5	0.5	1	1.5
B	0.14	0.15	0.38	0.3	0.15	0.22	0.26

	$Bi_{1.8}Sb_8$	$CoSb_3$	La_3Te_4	Bi_2Se_3	ZrNiSn
type	n	n	n	n	n
$T_{operate}$	150	850	1200	300	850
$\mu_0 m^{*3/2}$	400		10		150
N_v		3		1	
C_l		100			180
m_I^*		1.6		0.15	
Ξ		10			
κ_L	9	0.5	0.5	1.3	4.5
B	0.03	0.6	0.56	0.03	0.4

Adv. Mater. **24**, 6125 (2012)

37

Thermal effect on "the Energy Band Modification"

Temperature-dependent Hall coefficient (R_H)

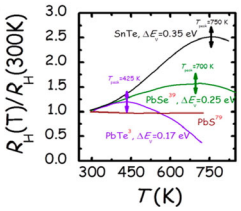

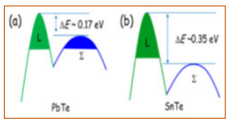

Hall coefficient (R_H, normalized relative to room-temperature value) for p-type SnTe, PbSe (39) and PbTe (3) show a strong temperature dependence indicative of a two-band conduction. The peaking temperature (T_{peak}) in the R_H-T curves is related to the magnitude of the energy difference (ΔE_v) between the two valence bands.

Ref: *J. Am. Chem. Soc.* **137**, 11507 (2015)

38

- **How are the carriers distributed in each of electronic bands ?**
- **How will this carrier distribution affect the thermoelectric properties ?**

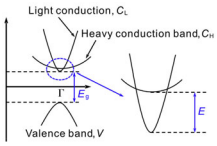

Three-band model for $Mg_2Sn_{0.75}Ge_{0.25}$

J. Materiomics, **2**, 203 (2016)

Band offset at 0K, Composition controllable

$$E = E_0 - T\frac{dE}{dT}$$

$$\xi_{C_H} = \xi_{C_L} - E/k_BT$$

Reduced Fermi energy in each band

$$n = 2\left(\frac{2\pi m^* k_B T}{h^2}\right)^{3/2} F_{1/2}(\xi)$$

39

Chemically-induced band convergence

Se → $\Delta E_{L\text{-}\Sigma}$ ↑ Mg → $\Delta E_{L\text{-}\Sigma}$ ↓

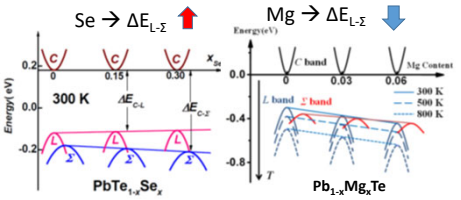

Increases T_{convg} Decreases T_{convg}

40

II. Stratagem of enhancing ZT

- ✓ Electronic band structure — band convergence
- ✓ **Reduction in thermal conductivity**

  Intrinsically low lattice κ , Defect Engineering
- ✓ Synergistically manipulating charge and phonon transports
- ✓ 3D charge and 2D phonon transports

41

Intrinsically low κ_L

$\kappa_{tot} = \kappa_L + \kappa_e$

Intrinsic low thermal conductivity is of practical interest due to its robustness against grain size, temperature range and other structural variations.

$$\kappa_L = \frac{1}{3} C_V v_g^2 \tau \qquad v_g = \frac{l}{\tau}$$

C_v : specific heat
v_g : group velocity
τ : phonon relaxation time

Low phonon group velocity | Large anharmonicity | Structure complexity

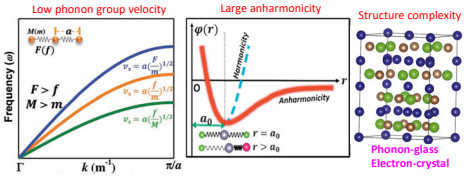

42

$$\kappa_L = \frac{1}{3} C_V v_g^2 \tau$$

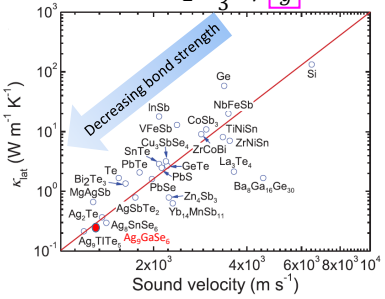

43

Ex:

Ag_9GaSe_6

"weakly bonded Ag"

κ_L ~ 0.15 W/m-K

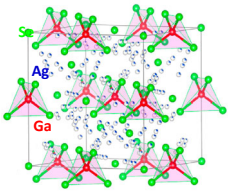

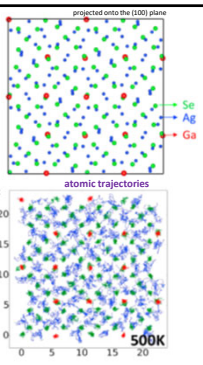

Joule,**1**, 816 (2017)

44

Anharmonicity

Although all bonding in real materials is anharmonic, the degree of anharmonicity varies strongly from material to material.

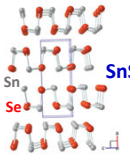

SnSe

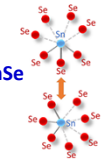

Asymmetry in vibration

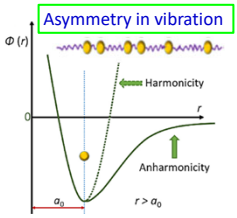

$$\kappa_L = \frac{1}{3} C_V v_g^2 \tau$$

Minimize τ by intensifying the scattering rate of phonons

45

Phonon – Phonon Umklapp scattering

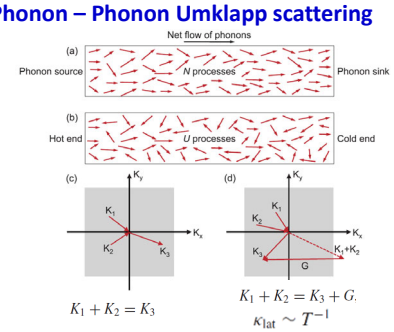

$K_1 + K_2 = K_3$

$K_1 + K_2 = K_3 + G$

$\kappa_{lat} \sim T^{-1}$

46

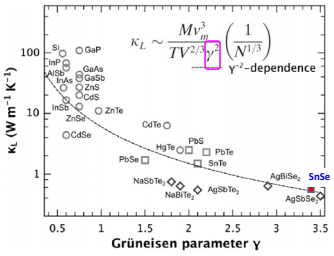

$$\gamma = -\frac{d\ ln\omega_i}{d\ lnV} = \frac{3\beta B V_m}{C_V}$$

Grüneisen parameter (γ):

- ✓ The rate of change of the vibrational frequency of a given mode with volume.
- ✓ To measure the strength of anharmonicity.

Angew. Chem. Int. Ed. **55**, 6826 (2016)

47

Complex crystal structure

$$\kappa_L = \frac{1}{3} C_V v_g^2 \tau$$

Compounds with a large number of atoms (*N*) in the primitive unit cell will exhibit low κ_L due to the large quantities of optical branches (*3N-3*).

Only a fraction of the heat can be transported by the limited acoustic branches: $C_V^a = C_V / N$

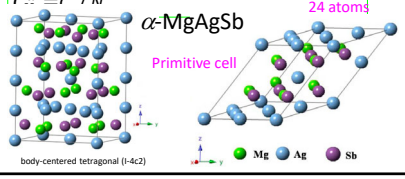

48

Acoustic Phonon v.s. Optical Phonon

- High Group velocity
- Only 3 modes per primitive cell
- Conduct most of heat

- Low Group velocity
- Have (3N-3) modes per primitive cell (large cells have many optical modes)
- Conduct less heat

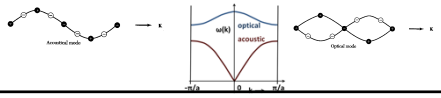

49

Complex crystal structure

$$\kappa_L = \frac{1}{3} C_V v_g^2 \tau$$

α-MgAgSb

N=24 → Acoustic branches: 3, Optical branches : 69

κ_L: 0.6 W/m-K

ZrNiSn

N=3 → Acoustic branches: 3, Optical branches : 6

κ_L:12 W/m-K

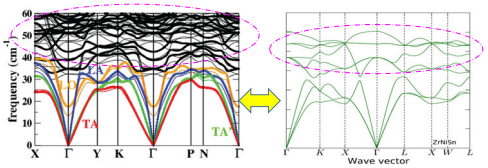

Energy Environ. Sci.,**11**, 23 (2018)

PRB, **95**, 045202 (2017)

50

Phonon modes : Acoustic & Optical

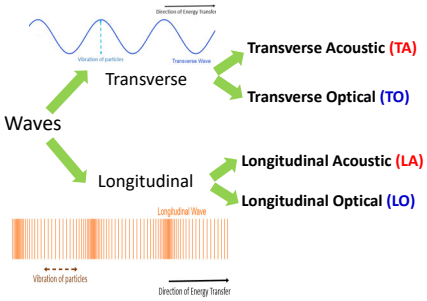

51

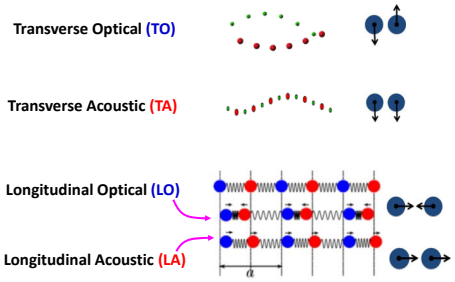

Images and movies from: Dr. *Taras Kolodiaynyi* & Dr. *Burak Himmetoglu*

52

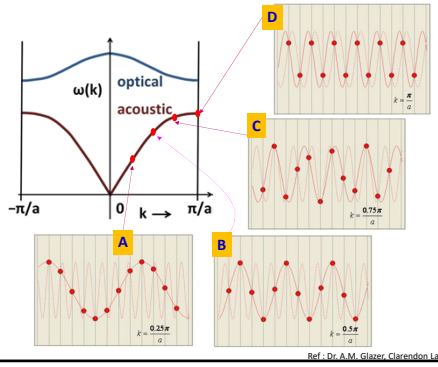

Ref : Dr. A.M. Glazer, Clarendon Laboratory

53

Acoustic and optical phonon coupling

The coupling between the acoustic and optical phonons will occasionally result in a substantial thermal resistance.

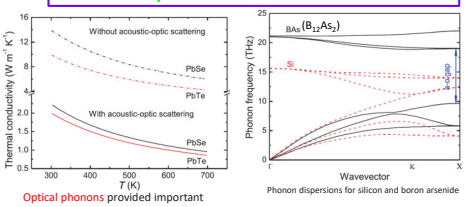

Optical phonons provided important scattering channels for acoustic phonons that were essential for the low κ.

Phonon dispersions for silicon and boron arsenide

BAs → ~ 1000 W/m-K
→ a negligible acoustic-optic phonon scattering
Si had a much smaller a–o gap
→ ~ 145 W/m-K

54

Defect engineering

$$\kappa_L = \frac{1}{3} C_V v_g^2 \tau$$

Phonon scattering by microstructural defects

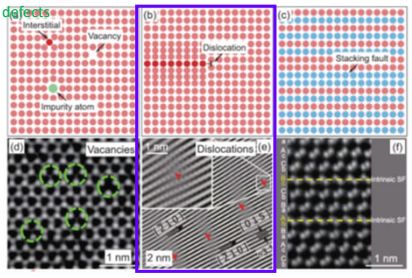

Ref: *Advances in Physics*, **67**, 69-147 (2018)

55

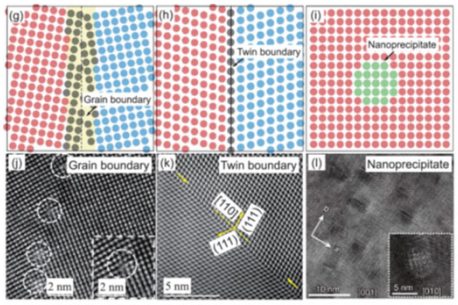

Ref: *Advances in Physics*, **67**, 69-147 (2018)

56

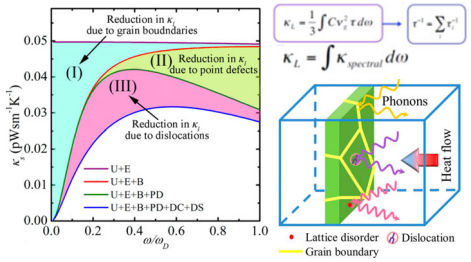

U: Umklapp process PD: Point defect
E: Electron DC: Dislocations core
B: Grain boundaries DS: Dislocation strains

57

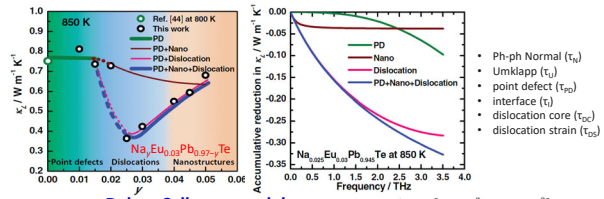

- Ph-ph Normal (τ_N)
- Umklapp (τ_U)
- point defect (τ_{PD})
- interface (τ_I)
- dislocation core (τ_{DC})
- dislocation strain (τ_{DS})

Debye-Callaway model

$$K_L = \frac{k_B}{2\pi^2 v}\left(\frac{k_B T}{\hbar}\right)^3 \int_0^{\theta_D/T} \tau_{tot}(x)\frac{x^4 e^x}{(e^x-1)^2}\,dx$$

$$\tau_{tot}^{-1} = \tau_U^{-1}+\tau_N^{-1}+\tau_{PD}^{-1}+\tau_{DC}^{-1}+\tau_{DS}^{-1}+\tau_I^{-1}$$

$$\tau_U^{-1} = \frac{2}{(6\pi^2)^{1/3}}\frac{k_B \bar{V}^{1/3}\gamma^2\omega^2 T}{\bar{M}v^3}$$

$$\tau_N^{-1} = \beta\,\tau_U^{-1}$$

$$\tau_{PD}^{-1} = \frac{V\omega^4}{4\pi v^3}\sum_i x_i\left[\left(\frac{M_i-\bar{M}}{\bar{M}}\right)^2+\varepsilon\left(\frac{a_i-\bar{a}}{\bar{a}}\right)^2\right]$$

$$\tau_{DC}^{-1} = N_D\frac{V^{4/3}}{v^2}\omega^3$$

$$\tau_{DS}^{-1} = A\times B_D^2 N_D \gamma^2\omega\left[\frac{1}{2}+\frac{1}{24}\left(\frac{1-2\nu}{1-\nu}\right)^2\left(1+\sqrt{2}\left(\frac{\eta_L}{\eta_T}\right)^2\right)^2\right]$$

$$\tau_I^{-1} = v\left[(2\pi R^2)^{-1}+\left(\pi R^2\frac{4}{\eta}(\Delta D/D)^2(\omega R/v)^4\right)^{-1}\right]^{-1}N_P$$

Ref: *Adv. Mater.* **29**, 1606768 (2017)

58

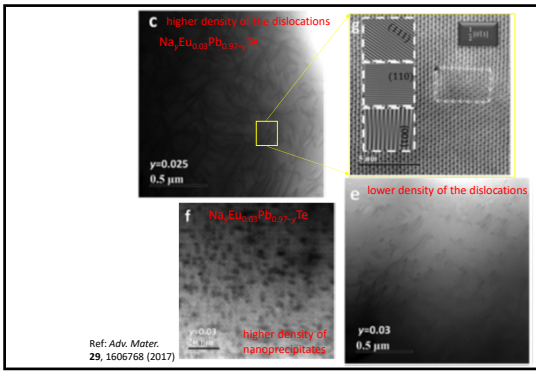

Ref: *Adv. Mater.* **29**, 1606768 (2017)

59

II. Stratagem of enhancing ZT

- ✓ Electronic band structure — band convergence
- ✓ Reduction in thermal conductivity

  Intrinsically low lattice κ , Defect Engineering
- ✓ **Synergistically manipulating charge and phonon transports**
- ✓ 3D charge and 2D phonon transports

60

Synergistically manipulating charge and phonon transports

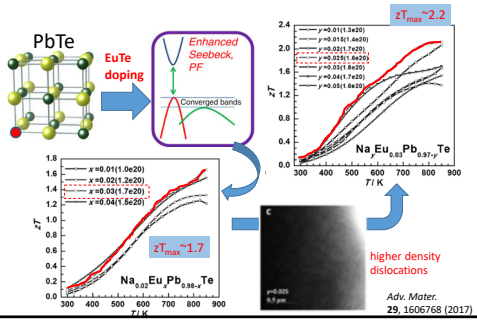

Adv. Mater. **29**, 1606768 (2017)

61

II. Stratagem of enhancing ZT

- ✓ Electronic band structure — band convergence
- ✓ Reduction in thermal conductivity

  Intrinsically low lattice κ , Defect Engineering
- ✓ Synergistically manipulating charge and phonon transports
- ✓ **3D charge and 2D phonon transports**

62

3D charge and 2D phonon transports

Science **360**, 778–783 (2018)

***n*-type SnSe crystals**

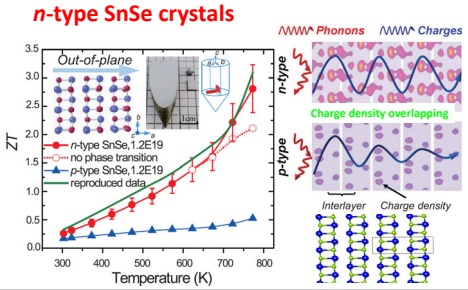

63

Outline

- I. Introduction to thermoelectrics
- II. Stratagem of enhancing ZT
- III. Sample Fabrication
- IV. ZT Measurements and characterization techniques
- V. Future works

$$ZT = \frac{S^2 \sigma T}{\kappa}$$

Sample Fabrication

- 1. Bulk Ingot, Polycrystal
- 2 Single crystal: Bridgmen method
- 3. Film : by deposition.

Categories: Sample Fabrication

1. Equilibrium processes :
   Crystal growth, melting & slow cooling,
   melting + long-time annealing,
   multi-step solid state reactions

2. Non-equilibrium processes :
   quench, mechanical alloying
   hot deformation, melt spinning
   self-propagating high-temperature synthesis

3. Spark plasma sintering (SPS)

Crystal growth of GeTe : Bridgman method

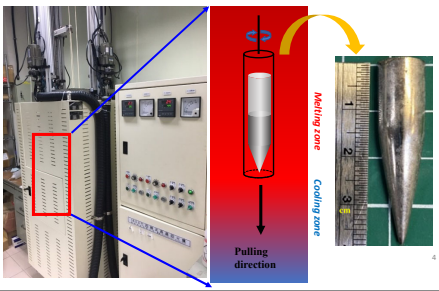

4. High Thermoelectric zT in GeTe Single Crystal with Sb Dopants

Synthesizing of $Ge_{1-x}Sb_xTe$ crystals

- The $Ge_{1-x}Sb_xTe$ crystals grown by Bridgman method that followed by a 2-step process.
- **1st step: pre-melting at high temperature**
  - Ge, Sb and Te are mixed by the stoichiometric ratio of high purity elements (99.999%)
  - Mixture sealed in the evacuated quartz ampoule under a vacuum of that better than 3×10^{-5} Torr.
  - The sealed mixture is pre-melted at high temperature for 48 hours
- **2nd step: Bridgman crystalizing**
  - Sealed in the sharp evacuated quartz ampoule under a vacuum of that better than 3×10^{-5} Torr.
  - Re-melting at melting zone.
  - Decline slowly at a rate of that <10 mm/hr into cooling zone.

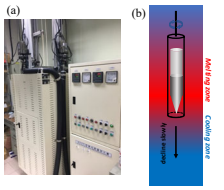

- The well known Bridgman method is employed to synthesize the antimony doped GeTe crystals.
  (a) The High temperature Bridgman furnace, right side the bulk material of a $Ge_{0.92}Sb_{0.08}Te$ crystal.
  (b) The interior temperature gradient of the vertical Bridgman furnace

$Ge_{1-x}Sb_xTe$

Fig.1

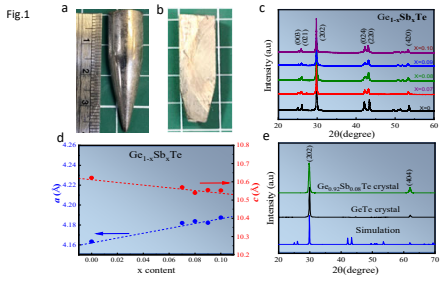

Growth of $Bi_xSb_{2-x}Te_3$ nanowires

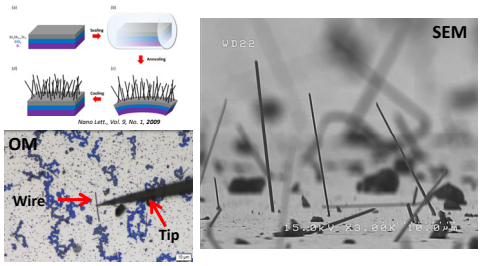

$Bi_{1.5}Sb_{0.5}Te_3$ thin film after annealing at 490℃ for 5 days

IV ZT Measurements and Characterization

Thermoelectric transport parameters

1. Seebeck coefficient
2. Thermal conductivity
3. Electrical resistivity

Measure uncertainty in ZT: $\frac{\Delta Z}{Z} = 2\frac{\Delta S}{S} + \frac{\Delta\sigma}{\sigma} + \frac{\Delta C_p}{C_p} + \frac{\Delta\lambda}{\lambda}$

$ZT = \frac{\sigma S^2}{\kappa}T \quad \kappa = \lambda\rho C_p$

1. Seebeck coefficient ($\frac{\Delta V}{\Delta T}$) and electrical conductivity

ZEM-3 Bulk, film

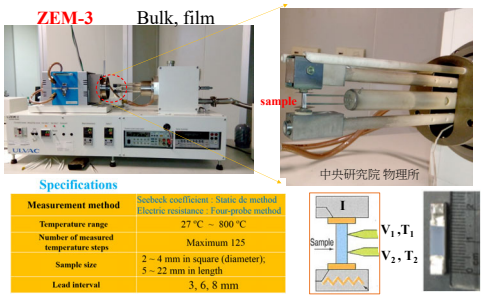

Specifications

Measurement method	Seebeck coefficient : Static dc method Electric resistance : Four-probe method
Temperature range	27 ℃ ~ 800 ℃
Number of measured temperature steps	Maximum 125
Sample size	2 ~ 4 mm in square (diameter); 5 ~ 22 mm in length
Lead interval	3, 6, 8 mm

Thermal conductivity measurement

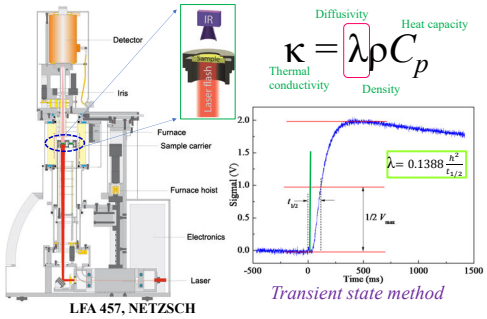

LFA 457, NETZSCH

Transient state method

Radiation Heat Loss Correction Model

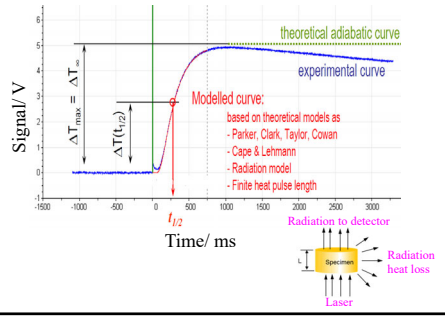

Sample Size

Thermal Diffusivity range	Possible sample thickness
Low diffusivity e.g. polymers (0.01-1 mm^2/s)	0.05 to 3 mm
Medium diffusivity e.g. ceramics (1-50 mm^2/s)	0.5 to 5 mm
High diffusivity e.g. copper (50-1200 mm^2/s)	1 to 5 mm

Inconel 600 (Standard Sample)

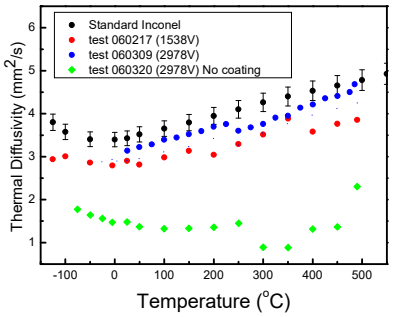

Pyroceram 9606 (Standard sample)

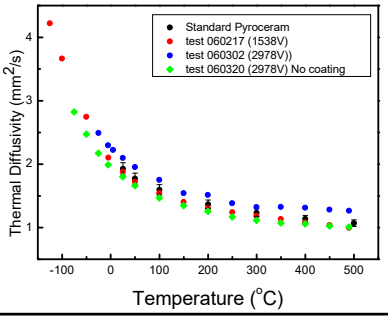

Pure Iron PR 41.01 (Standard Sample)

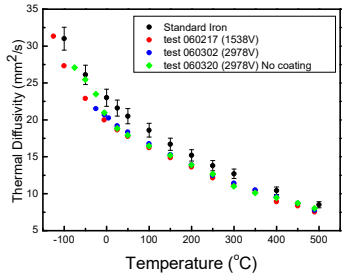

Thermal conductivity of thin films or tiny samples ?

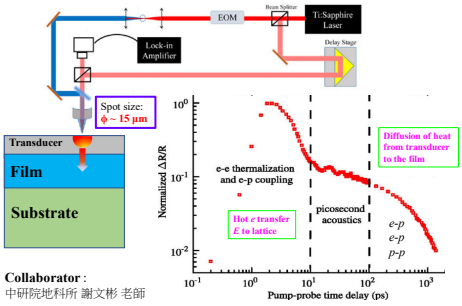

Collaborator :
中研院地科所 謝文彬 老師

16

Films at 300 K	S (μV/K)	σ (S/m)	κ (W/m-K)	PF(μW/m K²)	ZT
n type	- 230	27027	~ 0.4	1430	~ 1.0±0.1
p type	285	23809	~ 0.12	1933	2 ~ 3

Modulation Freq (MHz)	8.7	3.25	1.13	0.558
Thermal conductivity (W/m-K)	0.12	0.1	0.12	0.1

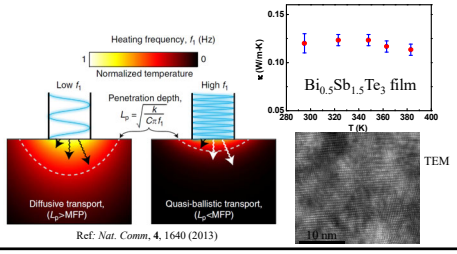

TEM

Ref: *Nat. Comm*, **4**, 1640 (2013)

17

Home-made thermoelectric measurement systems

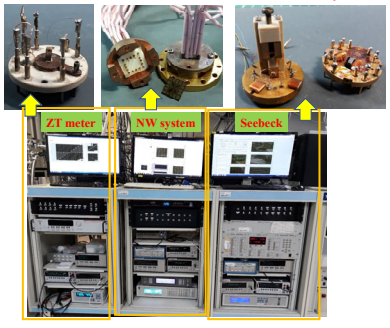

18

Seebeck , electrical resistivity

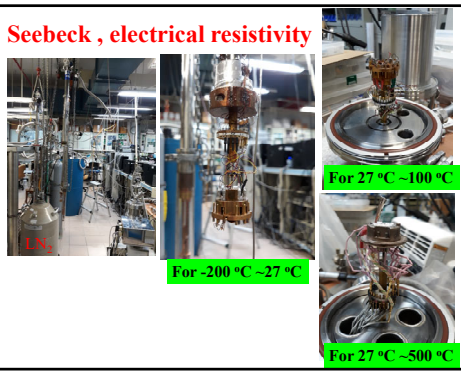

19

Seebeck and resistivity measure system 程式介面

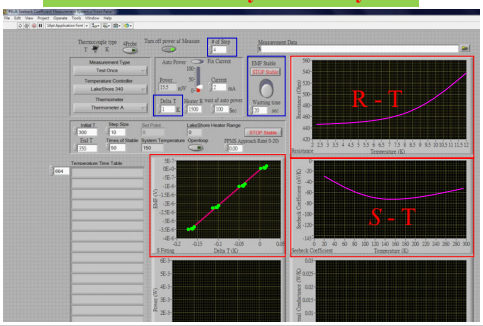

20

III. ZT measure platform for Nanowire

TE properties

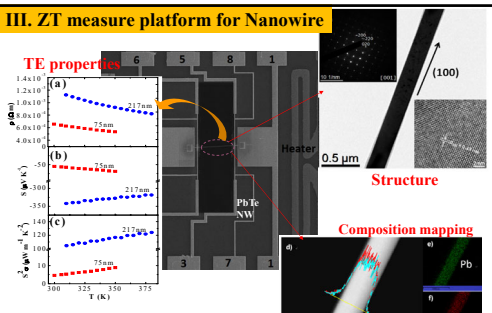

Structure

Composition mapping

"Stress-induced growth of single -crystalline lead telluride nanowires and their thermoelectric transport properties", *Appl. Phys. Lett.* **103**, 023115 (2013)

21

Design and Fabrications of N.W. measurement chip

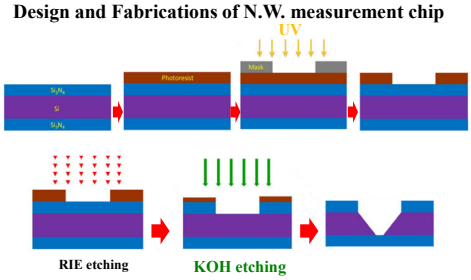

22

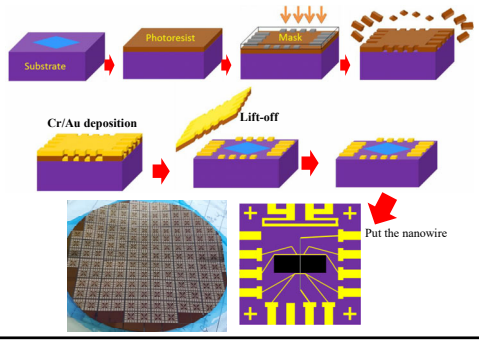

23

ZT Measurements, Specific Heat and Inelastic Neutron scattering

Low-Temperature heat capacity measurement (0.5 ~300 K)

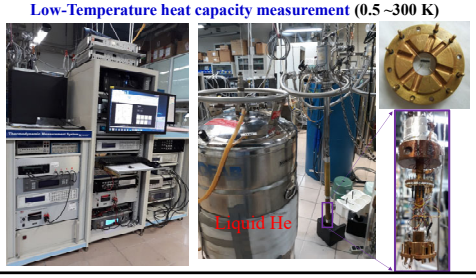

24

Reduction of lattice thermal conductivity by low energy **multi-Einstein optic modes**

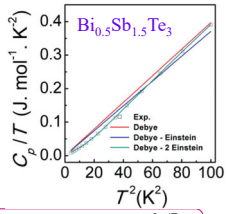

$$C_p/T = \gamma + \beta T^2 + \sum_{i=1}^{n} A_i(\Theta_{Ei})^2 (T^2)^{(-3/2)} \frac{e^{\Theta_{Ei}/T}}{(e^{\Theta_{Ei}/T}-1)^2}$$

Two Einstein oscillators with oscillation frequencies of 0.73 THz (35 K) and 1.29 THz (62 K) in the Debye host. The presence of the **high frequency phonon modes** that freeze out at the suitably low temperature which couple with the long wavelength acoustic phonon modes, resulting in an intrinsically low thermal conductivity in BiSbTe alloys.

25

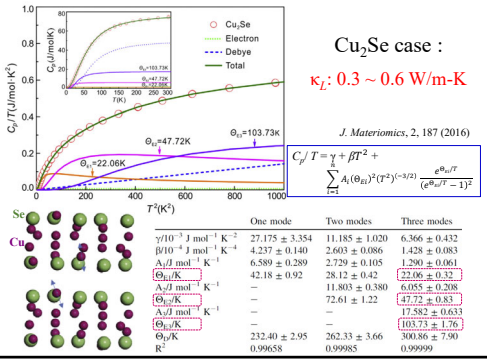

Cu$_2$Se case :

κ_L: 0.3 ~ 0.6 W/m-K

J. Materiomics, 2, 187 (2016)

$$C_p/T = \gamma + \beta T^2 + \sum_{i=1}^{n} A_i(\Theta_{Ei})^2 (T^2)^{(-3/2)} \frac{e^{\Theta_{Ei}/T}}{(e^{\Theta_{Ei}/T}-1)^2}$$

	One mode	Two modes	Three modes
γ/10^{-3} J mol^{-1} K^{-2}	27.175 ± 3.354	11.185 ± 1.020	6.366 ± 0.432
β/10^{-4} J mol^{-1} K^{-4}	4.237 ± 0.140	2.603 ± 0.086	1.428 ± 0.083
A_1/J mol^{-1} K^{-1}	6.589 ± 0.289	2.729 ± 0.105	1.290 ± 0.061
Θ_{E1}/K	42.18 ± 0.92	28.12 ± 0.42	22.06 ± 0.32
A_2/J mol^{-1} K^{-1}	–	11.803 ± 0.380	6.055 ± 0.208
Θ_{E2}/K	–	72.61 ± 1.22	47.72 ± 0.83
A_3/J mol^{-1} K^{-1}	–	–	17.582 ± 0.633
Θ_{E3}/K	–	–	103.73 ± 1.76
Θ_D/K	232.40 ± 2.95	262.33 ± 3.66	300.86 ± 7.90
R^2	0.99658	0.99985	0.99999

26

ZT Measurements, Specific Heat and **Inelastic Neutron scattering**

Thermal conductivity

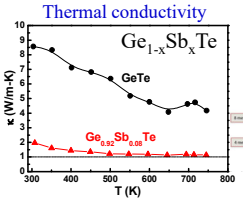

Phonon dispersion

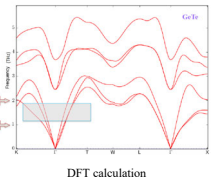

DFT calculation

27

Neutron instruments at ANSTO

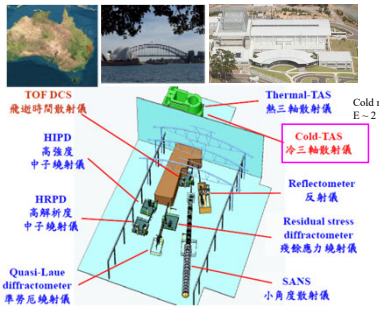

Cold neutron
E ~ 2 meV

28

View from atomic landscape

Elastic process

Momentum exchange: Yes
Energy exchange: No

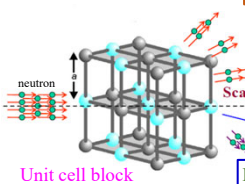

Inelastic process

Momentum exchange: Yes
Energy exchange: Yes

Momentum and energy changes of the probes

Understand the atomic arrangement and dynamics

29

How to measure phonon dispersion curves ?

Inelastic neutron scattering

If we can measure the energy lost by the neutron (by causing a vibration in the solid), and we can measure which direction you created the wave (wavevector, Q), then you can construct a phonon dispersion curve.

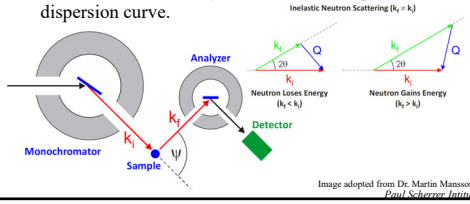

Image adopted from Dr. Martin Mansson
Paul Scherrer Intitut

30

Scan Parameters

SIKA - Cold Triple Axis neutron spectrometer

- GeTe
  - e = 0 ~ 12 meV
  - Γ → T
- $Ge_{0.92}Sb_{0.08}Te$
  - e = 0 ~ 12 meV
  - Γ → T

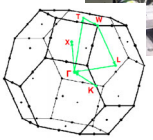

31

Γ → T
Q =1.0 ~ 1.5

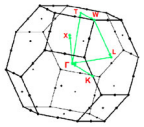

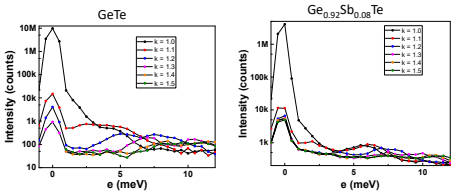

32

Γ → T
Q =1.0 ~ 1.5

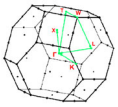

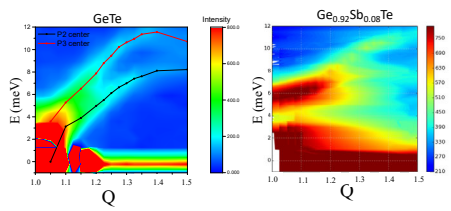

33

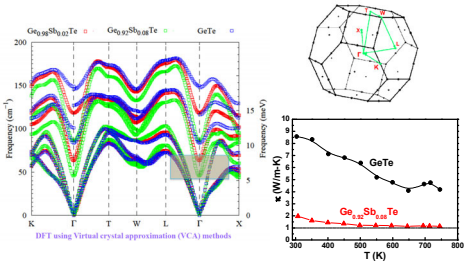

In the Γ point, $Ge_{0.92}Sb_{0.08}Te$ (green) have a phonon frequency around 6 meV (the shadow area) which cannot be seen from the pristine GeTe (blue) result. The overall phonon frequency got soften due to the Sb doping.

34

Outline

- Advances and prospect in GeTe-based materials
- Challenge and opportunity in GeTe
- Thermoelectric properties and phonon behavior in single crystals: GeTe , $(Ge_{1-x}Sb_x)Te$, $(Ge_{1-x}Bi_x)Te$ & $(Ge_{1-x-y}Bi_xSb_y)Te$
- Summary

$$ZT = \frac{S^2\sigma T}{\kappa}$$

Advances in GeTe-based materials

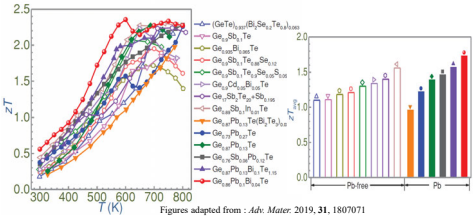

Figures adapted from : *Adv. Mater.* 2019, **31**, 1807071

- The high n_H, phase transition, multiple valence-bands, and resonant bonding make GeTe with diverse degrees of freedom to refine the thermoelectric performance.
- More importantly, a high **average *zT*** reaches ≈1.6 over a wide temperature region ranging from 300 to 800 K.

For practical applications

To ensure long and steady operation, thermoelectric materials are required to be mechanically robust !

Comparison of Vickers hardness

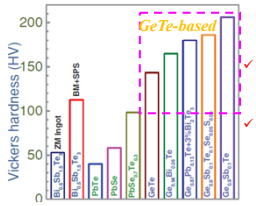

- ✓ GeTe-based materials demonstrate much higher Vickers hardness than Bi_2Te_3- and PbTe-based materials.
- ✓ Moreover, doping of Sb, Bi, and Pb can further enhance the Vickers hardness of GeT

Figures adapted from : *Adv. Mater.* 2019, **31**, 1807071

Band Structure Engineering

- ✓ Band degeneracy
- ✓ DOS resonant distortion near E_F

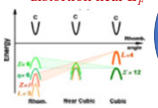

J. Am. Chem. Soc. 2018, **140**, 16190

n_H optimization & composition fluctuation

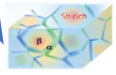

Adv. Mater. 2020, 2005612

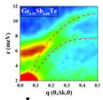

GeTe Challenges in Enhancing ZT

Phase transition

cubic GeTe via doping

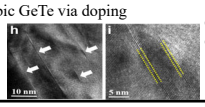

Reduction in κ

- Phonon velocity engineering
- Relaxation time engineering

$$\kappa_L = \frac{1}{3} C_V v_g^2 \tau$$

What are the advantages of single crystal GeTe-based materials ?

In some cases polycrystalline or single crystals show much better TE properties as compared to that of the melt ingots.

Many intrinsic physical properties of GeTe-based materials have not yet been extensively studied !

All samples were prepared either by quenching, melting, HP, SPS.....

Material	T [K]	S [μV K^{-1}]	σ [10^3 S cm^{-1}]	$S^2\sigma$ [μW cm^{-1} K^{-2}]	κ_L [W m^{-1} K^{-1}]	κ [W m^{-1} K^{-1}]	ZT
GeTe	300	34	0.87	10	1.5	6.3	0.1
GeTe	700	144	0.26	53	0.5	3.3	0.8
$Ge_{0.935}Bi_{0.065}Te$	700	236	–	34.7	1.08	1.51	1.8
$Ge_{0.87}Pb_{0.13}Te(Bi_2Te_3)_{0.03}$	770	270	0.77	35.5	1	2	1.9
$(GeTe)_{0.937}(Bi_2Sn_{0.2}Te_2)_{0.063}$	723	228	0.765	40	–	1.2	2.2
$Ge_{0.87}Pb_{0.13}Te$	687	192	1.074	40	0.4	1.2	2.3
$Ge_{0.75}Sb_{0.08}Pb_{0.17}Te$	800	265	0.463	32.5	0.5	1.1	2.3
$Ge_{0.85}Sb_{0.1}Pb_{0.05}Te$	736	256	0.542	35.6	0.5	1.2	2.3
$Ge_{0.85}Cd_{0.05}Bi_{0.10}Te$	650	231	0.77	41.6	0.5	1.2	2.3
$Ge_{0.84}Pb_{0.1}Bi_{0.06}Te$	600	287	0.365	30	0.48	0.63	2.4

Table adapted from : *Adv. Eng. Mater.* 2020, **10**, 2000367.

Thermal conductivity - 3ω method

$$V_{3\omega} \approx \frac{4I^3 LRR'}{\pi^4 \kappa S \sqrt{1+(2\omega\gamma)^2}}$$

I: Root mean squar value of $I_0 \sin \omega t$
L: Length of the nanowire between voltage contact
R: Electric resistance at the substrate temperature T_0
R': $(dR/dT)_{T_0}$
S: Cross section of the nanowire
γ: Thermal time constant

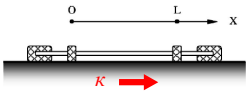

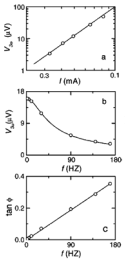

$V_{3\omega} \propto I^3$

$V_{3\omega} \propto \frac{1}{\sqrt{1+(2\omega\gamma)^2}}$

$\tan\phi \propto \omega$

L. Lu, W. Yi, and D. L. Zhang, *3ω method for specific heat and thermal conductivity measurements*, Rev. Sci. Instrum., **Vol. 72**, No. 7 (2001)

Thermal conductivity - 3ω method

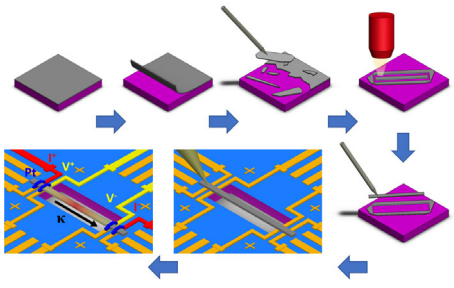

Thermal conductivity - 3ω method

$$V_{3\omega} \approx \frac{4I^3 LRR'}{\pi^4 \kappa S \sqrt{1+(2\omega\gamma)^2}}$$

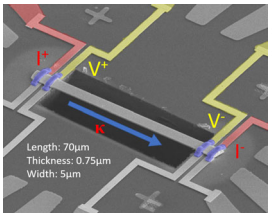

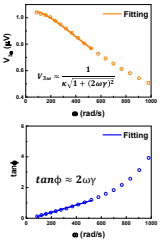

Thermal conductivity

Confirm the 3ω measurement of thermal conductivity in the film

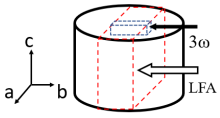

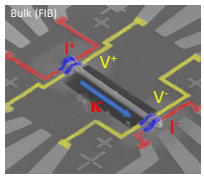

Length: 65μm
Thickness: 1.5μm
Width: 3μm

43

Thermal conductivity

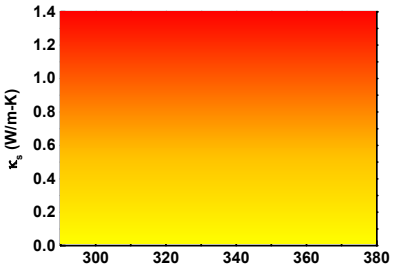

44

Conclusions and future work

- ✓ $Bi_{0.5}Sb_{1.5}Te_3$ thin films were deposited on glass substrates at a temperature of 200˚C using a sputtering device. Te annealing
- ✓ The piece of a specimen is obtained from the artificial scratched thin film that further processed as a belt sample by following the focused ion beam (FIB) treatment.
- ✓ The in-plane thermal conductivity of thin-film successfully measured by the 3ω method.
- ✓ These heterointerfaces among $Bi_{0.5}Sb_{1.5}Te_3$ is randomly distributed in the film and may help to achieve an optimized carrier transport and a lower thermal conductivity.
- ✓ The measurement result shows ultralow thermal conductivity ~ 0.28 W/m-K and ZT ≈ 1.8 for the 0.5 μm-thick $Bi_{0.5}Sb_{1.5}Te_3$ thin-film at 340K.

45

Example 2

ADVANCED SCIENCE
www.advancedscience.com

High *zT* and Its Origin in Sb-doped GeTe Single Crystals

Ranganayakulu K. Vankayala, Tian-Wey Lan, Prakash Parajuli, Fengjiao Liu, Rahul Rao, Shih Hsun Yu, Tsu-Lien Hung, Chih-Hao Lee, Shin-ichiro Yano, Cheng-Rong Hsing, Duc-Long Nguyen, Cheng-Lung Chen, Sriparna Bhattacharya,* Kuei-Hsien Chen, Min-Nan Ou, Oliver Rancu, Apparao M. Rao, and Yang-Yuan Chen**

Advanced Science, Vol. 7, 2002494 (2020)

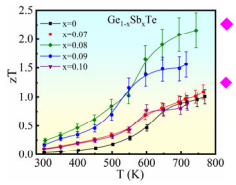

- A record high ***zT* of 2.2** at 740 K is reported in $Ge_{0.92}Sb_{0.08}Te$ crystals.
- Additional **phonon excitations** are discovered in $Ge_{0.92}Sb_{0.08}Te$ and help soften the phonon frequencies !

Inelastic neutron scattering studies of GeTe and $Ge_{0.92}Sb_{0.08}Te$

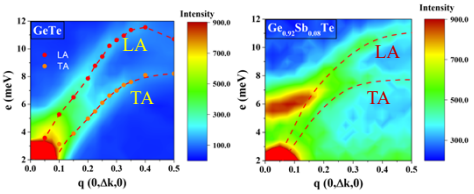

- ➢ Highlight the greater complexity of the phonon dispersion of Ge0.92Sb0.08Te compared to that of GeTe.
- ➢ An unexpected extra excitation between **5~7 meV** is observed in the $Ge_{0.92}Sb_{0.08}Te$ crystal.

Phonon density of state (PDOS)

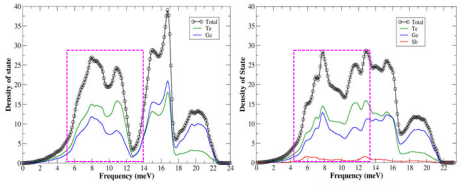

The results of PDOS show additional features between ≈ 5–7 and ≈12–13 meV for GST. We attribute these features to the presence of Sb dopants.

Phonon density of state (PDOS)

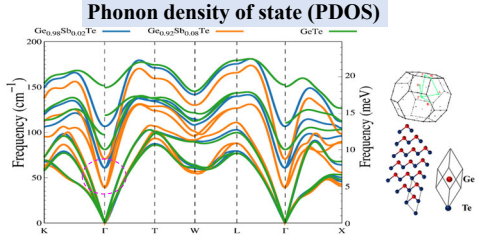

- The overall phonon frequency got soften due to the Sb doping. For GeTe, in the Γ point, it cannot be found any phonon mode between 0~10 meV.
- The presence of a phonon ~ **5 meV** at the Γ point can clearly be seen in the dispersion of $Ge_{0.92}Sb_{0.08}Te$ (orange traces), which could provide extra decay channels for optical phonons, thereby increasing their scattering rate and lowering the thermal conductivity !

Phonon transport

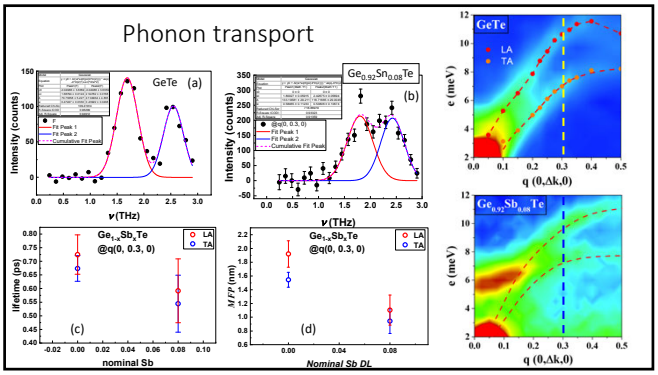

Diverse microstructures, *i.e.*, planar defects, stacking faults, are observed in $Ge_{0.92}Sb_{0.08}Te$, and are expected to enhance multiple scattering of phonons !

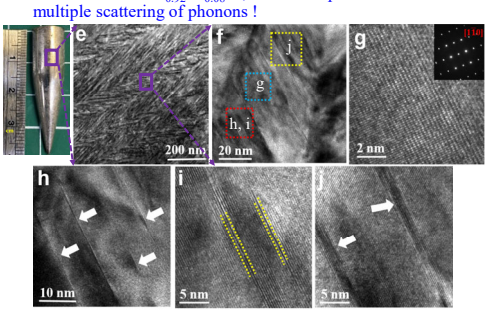

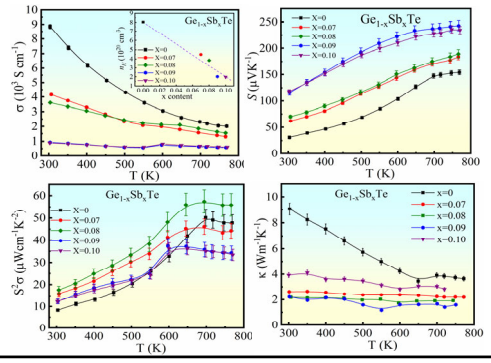

Spark plasma sintering

A strategy to optimize the thermoelectric performance in spark plasma sintering process

1. Spark plasma sintering (SPS) is, nowadays, widely applied to existing alloys as a means of further enhancing the alloys' figure of merit.
2. However the **optimal sintering condition** is difficult to determine, and for the most part, is based on experiences.
3. We demonstrates a systematic way to independently optimize the Seebeck coefficient S and the ratio of electrical to thermal conductivity (σ/κ), and through this, achieve the maximum figure of merit $zT = S^2(\sigma/\kappa)T$.

Detail information : *Scientific Reports*, 6, 23143 (2016)

Spark Plasma Sintering

SPS-515S, SPS SYNTEX INC
(中央研究院 物理研究所)

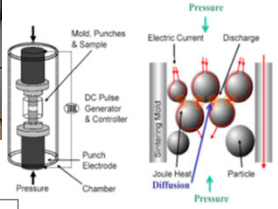

Images: Prof. Guoqiang Xie (Tohoku University, Japan)

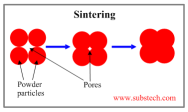

T > 1000 °C

Guillon *et al.*

Spark plasma sintering process

Densification process is a temperature dependent mass transport process that involves surface diffusion, evaporation, grain boundary diffusion and interparticle neck formation.

✓Temperature
✓Pressure

Heating rate
Holding time

	573 K	623 K	673 K
50 MPa	zT ?	density ?	
100Mpa			

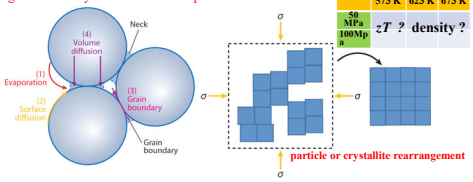

To achieve effective densification, the sintering parameters should be tuned to favour densification over coarsening !

55

Thermal conductivity - 3ω method

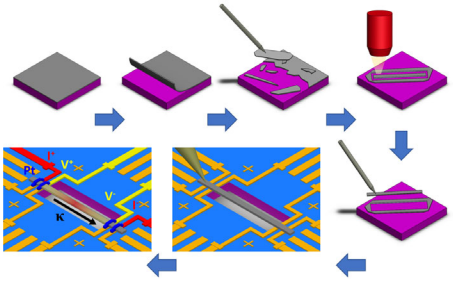

56

Thermal conductivity - 3ω method

Wei-Han Tsai (蔡瑋瀚)

$$V_{3\omega} \approx \frac{4I^3LRR'}{\pi^4 \kappa S\sqrt{1+(2\omega\gamma)^2}}$$

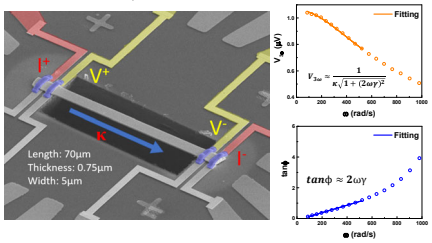

57